



# Photocatalytic degradation rate of oxalic acid on a semiconductive layer of $n$ -TiO<sub>2</sub> particles in a batch mode plate photoreactor

## Part II: Light intensity limit

J. KRÝSA<sup>1\*</sup>, L. VODEHNAL<sup>1</sup> and J. JIRKOVSKÝ<sup>2</sup>

<sup>1</sup>Institute of Chemical Technology, Department of Inorganic Technology, Technická 5, 166 28 Prague 6, Czech Republic

<sup>2</sup>J. Heyrovský Institute of Physical Chemistry, Academy of Sciences, Dolejškova 3, 182 23 Prague 8, Czech Republic

(\*author for correspondence, e-mail: krytaj@vscht.cz)

Received 30 March 1998; accepted in revised form 18 August 1998

The effect of light intensity, flow rate and oxygen bubbling on the photocatalytic degradation rate of oxalic acid on a layer of TiO<sub>2</sub> particles was investigated. At higher concentrations of oxalic acid ( $\geq 0.005$  M) and photon flux intensity in the range  $3.26 \times 10^{-10}$  to  $1.07 \times 10^{-8}$  einstein cm<sup>-2</sup> s<sup>-1</sup>, the rate of photocatalysis was controlled simultaneously by the flux of both oxygen and photons. This is probably caused by the ability of oxygen to react with photogenerated electrons and thus suppress the electron-hole recombination and increase the efficiency of the photocatalytic degradation.

Keywords: photocatalytic degradation, oxalic acid,  $n$ -TiO<sub>2</sub>, light intensity

### List of symbols

$A$	active surface of the reactor plate (7200 cm <sup>2</sup> )
$c$	concentration (mol cm <sup>-3</sup> )
$c_1$	velocity of the light ( $3.0 \times 10^{10}$ cm s <sup>-1</sup> )
$D$	diffusion coefficient (cm <sup>2</sup> s <sup>-1</sup> )
$h$	Planck constant ( $6.6262 \times 10^{-34}$ J s)
$I$	intensity of u.v.-light (W cm <sup>-2</sup> )
$J$	flux density (mol cm <sup>-2</sup> s <sup>-1</sup> ) or (einstein cm <sup>-2</sup> s <sup>-1</sup> )
$L$	length of the reactor plate (cm)
$n$	molar amount (mol)
$N_A$	Avogadro constant ( $6.022 \times 10^{23}$ mol <sup>-1</sup> )
$Q$	flow-rate (cm <sup>3</sup> s <sup>-1</sup> )
$V_r$	total volume of the solution (15 000 cm <sup>3</sup> )
$w$	width of the reactor plate (cm)

### Greek symbols

$\alpha$	inclination angle of the reactor plate to the horizontal
$\lambda$	wavelength of the light (cm)
$\tau$	time (s)
$\Gamma$	photon yield (%)

### Subscripts

(COOH) <sub>2</sub>	oxalic acid
$h\nu$	photons
lim	limiting
N	Nernst
O <sub>2</sub>	oxygen
org	organic compound

### Superscripts

0	bulk
s	surface

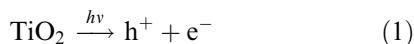
### 1. Introduction

The degradation of organic toxic compounds such as PCBs, phenols and pesticides dissolved in water is a significant problem because, due to their toxicity, a common biological treatment cannot often be used. These substances are mostly adsorbed on active carbon and then burned at high temperature, a process which may produce highly toxic pollutants. This is the reason for the development of methods making

use of extremely reactive radicals, capable of destroying organic, and some inorganic, pollutants. Examples of such methods are homogeneous photolysis, heterogeneous photocatalysis, radiolysis and indirect electrolysis [1].

The heterogeneous photocatalytic system consists of semiconductive particles, which act as photocatalyst in contact with the reaction medium. Irradiation of the semiconductor (e.g. TiO<sub>2</sub>) with photons of energy,  $h\nu$ , greater than the bandgap

energy generates charge carrier pairs, positive holes and electrons



The charge carriers react on the photocatalyst surface with molecules of an acceptor and of a donor if their redox potentials lie within the bandgap. However, before the electrons and holes reach the surface, they may undergo recombination, which is generally responsible for low efficiency in systems employing semiconductor catalysts for photochemical conversion of light energy [2].

Hoffmann *et al.* [3] described variables important in determining the reaction rate and extent of transformation during photocatalytic degradation. They include the semiconductor concentration, the reactive surface area and porosity of the photocatalyst aggregates, the concentrations of both donors and acceptors, the incident light intensity, the pH, the presence of competitive sorbates and the temperature.

Trillas *et al.* [4] investigated the photocatalytic oxidation of phenoxyacetic acid in illuminated suspension of  $\text{TiO}_2$ . They found that the degradation rate was proportional to the square root of the light intensity. This indicates that the electron-hole recombination process is an important event and that the energy efficiency is low.

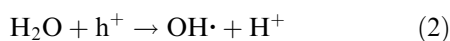
Kormann *et al.* [5] studied the photocatalytic degradation of chloroform in aqueous suspensions of  $\text{TiO}_2$ . The quantum efficiency of the photo degradation of  $\text{CHCl}_3$  ( $\Gamma = 0.56\%$  at  $\lambda = 330$  nm and photon flux  $2.8 \times 10^{-6}$  einstein  $\text{dm}^{-3} \text{min}^{-1}$ ) was found to be inversely proportional to the square root of the incident light intensity.

Recently Butterfield *et al.* [6] used a falling film reactor consisting of stainless steel pipe coated on the inside surface with  $\text{TiO}_2$  sol-gel film for photocatalytic degradation of organic pollutants. The film was illuminated by an ultraviolet light tube inserted down the axis of the vertical pipe. The disadvantage of this photoreactor is that it cannot work under natural sun light.

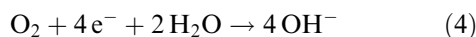
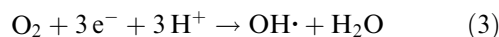
This work is a continuation of a previous study which was devoted to the influence of mass transfer rate of both oxygen and oxalic acid on the degradation of oxalic acid in liquid film which circulated over a semiconductive layer of titanium dioxide particles on a glass plate [7]. The aim is an investigation of the light intensity effect on the photocatalytic degradation rate of oxalic acid and a critical discussion of three previously postulated limiting cases [7].

## 2. Theory

A typical characteristic of semiconductive metallic oxides is the extremely high oxidative potential of the holes. This enables one electron oxidation of water with the generation of a strongly oxidative hydroxyl radical ( $\text{OH}\cdot$ ) [1].



Equation 2 states that a hole reacts with water with the formation of one hydroxyl radical. This radical, bound to the semiconductor surface, is a chemical equivalent to the surface trapped hole [8]. The hydroxyl radical is able to react with almost all organic molecules and thus to initiate the oxidative degradation. The dissolved oxygen generally acts as an electron acceptor. In previous work [7] the mechanism of the reaction of  $\text{O}_2$  with an electron was described and it was reported that the consumption of one molecule of oxygen is connected with the consumption of three or four electrons:



The mechanism of the reaction of oxalic acid with hydroxyl radical ( $\text{OH}\cdot$ ) can be described by the following equations



Two  $\cdot\text{COOH}$  radicals either recombine with the formation of oxalic acid,



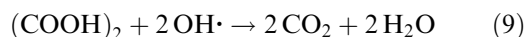
or disproportionate with the formation of carbon dioxide and formic acid:



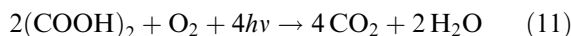
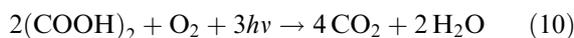
Formic acid further reacts with the hydroxyl radical ( $\text{OH}\cdot$ ) as follows



Considering Reactions 5, 6 and 7(a) or 5, 6, 7(b) and 8, gives the same overall reaction for oxidation of oxalic acid by hydroxyl radicals



Combining Equations 1, 2, 9 and 3 or 4, overall equations describing the total oxidation of oxalic acid can be obtained:



On the one hand, Equations 10 and 11 describe the photocatalytic oxidation of oxalic acid via consumption of a different number of photons (3/2, 4/2) per molecule of oxalic acid. On the other hand, the consumption of oxygen molecules (1/2) per molecule of oxalic acid is the same for both the above mentioned equations. The stoichiometric coefficient for  $h\nu$  and  $\text{O}_2$  in Equations 10 and 11 will be denoted as  $\nu_{h\nu}$  and  $\nu_{\text{O}_2}$ , respectively.

## 3. Experimental details

The plate solar reactor (Fig. 1) was described previously [7]. The only change was that the parallel plate with 10 ultraviolet sun bed bulbs (Osram Eversun L40W/79K) was mounted above the glass plate at a

distance of 10.5 cm (in some cases at 110 cm). The preparation of the TiO<sub>2</sub> layer (Degussa P 25) was similar to that proposed by Bockelmann [9] and was also, together with the oxalic acid determination, described previously [7].

## 4. Results and discussion

### 4.1. Determination of the photon flux

The light intensity on the reactor plate was measured photometrically (photometer/radiometer model 450 with a 550-2 type C multiprobe detector, EG&G, USA). Light intensities for a different number of tubes mounted on the parallel plate at a distance of 110 cm above the glass plate with TiO<sub>2</sub> are represented in Fig. 2. They were measured along the longer axis of the photocatalyst plate. It is apparent that the light intensity increased with the number of tubes and was relatively regularly distributed. A slight decrease in the light intensity due to the geometry of tubes was observed at both ends of the plate. An average light intensity (for a particular number of sunbed tubes) was calculated using 20 values of light intensity measured at different positions of the reactor plate.

An average photon flux,  $J_{hv}$  (einstein mol<sup>-1</sup> cm<sup>-2</sup>), was calculated from the average light intensity,  $I$  (μW cm<sup>-2</sup>) by the equation

$$J_{hv} = \frac{I\lambda_m}{c_1 N_A h} \quad (12)$$

where  $c_1$ ,  $N_A$ ,  $\lambda$  are listed at the outset and  $\lambda_m$  is the wavelength corresponding to the maximum emission of the sun bed tubes ( $3.55 \times 10^{-5}$  cm).

### 4.2. Balance equations for a plate reactor in batch mode

The degradation flux density of an organic compound,  $J_{org}$  (mol cm<sup>-2</sup> s<sup>-1</sup>), in a batch mode reactor can be expressed in differential form as

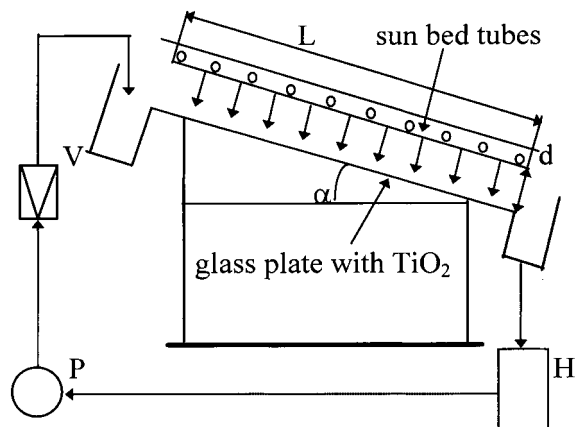


Fig. 1. Schematic representation of the batch mode plate photoreactor with a flow of the solution. Description: (H) holding tank, (P) pump, (V) Venturi tube, (d) a distance between the sun bed tubes and the glass plate with TiO<sub>2</sub> (10.5 or 110 cm), (L) length of the reactor plate (120 cm), ( $\alpha$ ) inclination angle (10°).

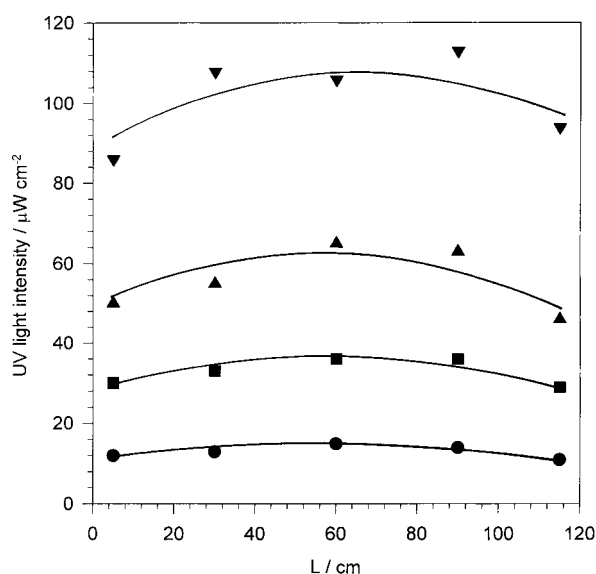


Fig. 2. Dependence of light intensity distribution along length of plate photoreactor on the number of sun bed tubes (placed at a distance 110 cm above the plate with TiO<sub>2</sub>). Key: (●) 1 tube, (■) 3 tubes, (▲) 5 tubes, (▼) 10 tubes.

$$-|J_{org}| = \frac{V_r}{A} \frac{dc_{org}}{d\tau} \quad (13)$$

The volume of liquid covering the reactor plate  $V_p$  is negligible in comparison with the total volume of liquid  $V_r$ . A well mixed liquid circulates over the plate with a volumetric flow rate  $Q$ . Owing to a relatively high volumetric flow rate, the concentration changes of the organic compound in the liquid film along the reactor plate are negligible in comparison with the bulk concentration of that compound. In the previous paper [7] the calculation of the decrease in oxalic acid in the flowing film was described. Using the same approach it was calculated that for a flow rate of  $42 \text{ cm}^3 \text{ s}^{-1}$  the average flowing film thickness was 0.49 mm and the oxalic acid concentration change was  $0.83 \times 10^{-4} \text{ mol dm}^{-3}$ . For an oxalic acid concentration in the holding tank of 0.005 and 0.001 mol dm<sup>-3</sup> the concentration change is about 1.6% and 8.4%, respectively.

The molar flux of photons,  $J_{hv}$ , used for the photodegradation of oxalic acid follows from the stoichiometry of Reaction 11

$$J_{hv} = \frac{v_{hv}}{v_{org}} |J_{org}| \quad (14)$$

Similarly, the flux density of oxygen,  $J_{O_2}$ , is given by

$$|J_{O_2}| = \frac{v_{O_2}}{v_{org}} |J_{org}| \quad (15)$$

The limiting flux density is defined for the case when the concentration of the species (oxygen or organic compound) at the surface of the  $n$ -TiO<sub>2</sub> layer decreases to zero due to the photocatalytic reaction. Depending on the values of the limiting flux densities of all, oxygen, oxalic acid and photons, three different limiting cases given by the following conditions can be considered:

- (i)  $|J_{O_2,lim}| \ll \frac{1}{v_{hv}} J_{hv}$  and  $|J_{O_2,lim}| \ll \frac{1}{v_{org}} |J_{org,lim}|$   
(ii)  $\frac{1}{v_{org}} |J_{org,lim}| \ll |J_{O_2,lim}|$  and  $\frac{1}{v_{org}} |J_{org,lim}| \ll \frac{1}{v_{hv}} J_{hv}$   
(iii)  $\frac{1}{v_{hv}} J_{hv} \ll |J_{O_2,lim}|$  and  $\frac{1}{v_{hv}} J_{hv} \ll \frac{1}{v_{org}} |J_{org,lim}|$

The consumption of photons per mole of electron scavenger (oxygen) and per molecule of organic compound (oxalic acid) forms the background of the calculation. The development of equations for mass transfer coefficient which permits the calculation of the limiting flux density was reported in the first part of the paper [7]. The analysis was performed for a model compound, oxalic acid, but is also applicable for other organic compounds providing the consumption of photons and electron scavenger (oxygen) per molecule of organic compound is known. The multiplying coefficients in Equations 14–16 and 19 follows from the stoichiometry of the Equation 11 ( $v_{hv} = 4$ ,  $v_{org} = 2$  and  $v_{O_2} = 1$ ).

Case (i) describes the situation, when the flux density of photons and of oxalic acid to the photocatalyst plate are sufficiently high and the flux density of oxygen is a limiting factor. Introducing Equation 15 into Equation 13 and integrating gives a linear decrease of the organic compound concentration with irradiation time

$$c_{org}^0(\tau) = c_{org}^0(0) - 2 \frac{A}{V_r} |J_{O_2,lim}| \tau \quad (16)$$

Case (ii) is valid for a very low bulk concentration of oxalic acid. The flux density of photons and of oxygen are significantly higher than the limiting flux density of oxalic acid. Due to the photocatalytic reaction the concentration of oxalic acid on the photocatalyst surface ( $c_{org}^S$ ) should be equal to zero. Then  $J_{org,lim}$  may be expressed as

$$J_{org,lim} = -D_{org} \frac{c_{org}^0}{\delta_{N,org}} \quad (17)$$

From the integration of Equation 13 it follows that the concentration of oxalic acid decreases exponentially with irradiation time.

Cases (i) and (ii) were studied in detail in the previous work [7]. The effect of flow rate and oxygen bubbling on the degradation rate of  $(COOH)_2$  were investigated at a constant photon flux density,  $J_{hv} = 1 \times 10^{-8}$  einstein  $cm^{-2} s^{-1}$ , and for initial oxalic acid concentrations in the range from 0.0025 to 0.01 M (case (i)) and 0.0001 M (case (ii)). It was found that the degradation rate of oxalic acid increased with increasing flow rate and with increase in the oxygen concentration (bubbling of the holding tank with oxygen). It was concluded, in agreement with other works [10–12], that the photocatalytic degradation was controlled by the mass transport of both substances ( $(COOH)_2$ ,  $O_2$ ) participating in the photocatalytic reactions on the  $TiO_2$  surface. The degradation flux density of oxalic acid was calculated from the observed concentration decay (Equation 13). The

limiting flux density of oxygen to the  $TiO_2$  surface was calculated by

$$J_{O_2,lim} = -D_{O_2} \frac{c_{O_2}^0}{\delta_{N,O_2}} \quad (18)$$

where  $D_{O_2}$  is the diffusion coefficient of oxygen,  $c_{O_2}^0$  the oxygen concentration in the solution and  $\delta_{N,O_2}$  the Nernst diffusion layer thickness.  $\delta_{N,O_2}$  was calculated for the given hydrodynamic conditions (flow rate, viscosity, inclination and width of the plate). The theoretical degradation flux density of oxalic acid was calculated from the limiting flux density of oxygen (Equation 15) assuming that the rate of photocatalysis is controlled by the transport of oxygen to the photocatalyst surface. The experimentally measured (Equation 13) and theoretically calculated (Equation 15) degradation flux densities of oxalic acid were in a good agreement which showed that the rate of photocatalysis was controlled by the transport of oxygen to the photocatalyst surface in the concentration range 0.0025 to 0.01 M  $(COOH)_2$  and for the photon flux density ( $1 \times 10^{-8}$  einstein  $cm^{-2} s^{-1}$ ) [7].

Case (iii) is similar to case (i). Replacing  $J_{O_2,lim}$  in Equation 20 by  $\frac{1}{2} J_{hv}$  we obtain

$$c_{org}^0(\tau) = c_{org}^0(0) - \frac{1}{2} \frac{A}{V_r} J_{hv} \tau \quad (19)$$

which shows that the concentration decreases linearly with irradiation time.

#### 4.3. Effect of the light intensity

The dependence of degradation rate on the light intensity was studied with the aim of confirming the limiting effect of the photon flux. Figure 3 shows the decrease in the oxalic acid concentration with irradiation time for various photon flux densities and for a constant flow rate of 2.5  $dm^3 min^{-1}$ . The depen-

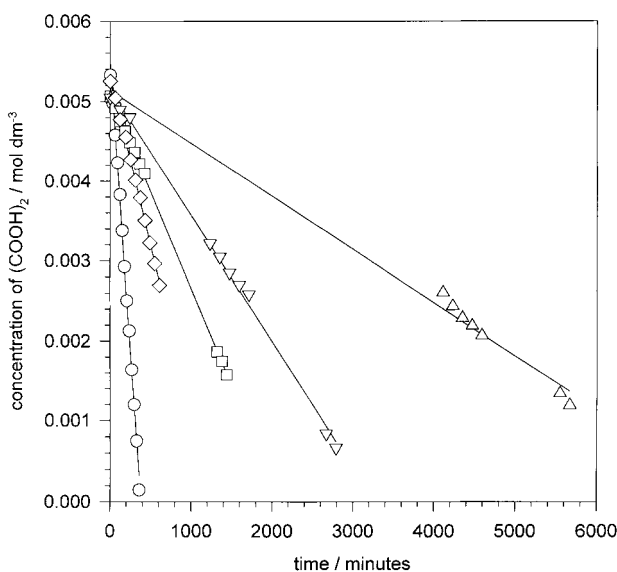


Fig. 3. Dependence of oxalic acid concentration on irradiation time for different photon flux intensities. Flow rate 2.5  $dm^3 min^{-1}$ ,  $V_r = 15 dm^3$ . Photon flux density /  $10^{-10}$  einstein  $cm^{-2} s^{-1}$ : (○) 107, (◇) 25.6, (□) 15.1, (▽) 8.9 and (△) 3.26.

dencies are linear for all photon flux densities, which confirms the theoretical assumption that the rate of photocatalysis is controlled either by the oxygen flux (Equation 16, case (i)) or by the photon flux (Equation 19, case (iii)). The dependence of photocatalysis rates (slopes  $dc/d\tau$ ) on the photon flux density is shown in Fig. 4 for two different flow rates. The rate increases linearly for lower photon flux densities while for values higher than approximately  $2.5 \times 10^{-9}$  einstein  $\text{cm}^{-2} \text{s}^{-1}$ , the increase in reaction rate is slower. The enhancement of the photocatalysis rate by flow rate and by oxygen bubbling (Fig. 5) depended on the light intensity. For the photon flux density  $1.07 \times 10^{-8}$  einstein  $\text{cm}^{-2} \text{s}^{-1}$ , the photocatalysis rate increased with change of flow rate (from  $2.5 \text{ dm}^3 \text{ min}^{-1}$  to  $3.2 \text{ dm}^3 \text{ min}^{-1}$ ) by 15% while for  $3.26 \times 10^{-10}$  einstein  $\text{cm}^{-2} \text{s}^{-1}$  it increased by 45%. The photocatalysis rate increased with the oxygen bubbling by 55% ( $1.07 \times 10^{-8}$  einstein  $\text{cm}^{-2} \text{s}^{-1}$ ) while for the photon flux density  $3.26 \times 10^{-10}$  einstein  $\text{cm}^{-2} \text{s}^{-1}$  it increased only by 20%. It seems that the influence of flow rate decreases while that of oxygen bubbling (increase of oxygen concentration) increases with increasing photon flux density.

It follows from Figs 4 and 5 that the degradation rate is controlled by the photon flux density and by the oxygen diffusion from the bulk of the flowing liquid film to the  $\text{TiO}_2$  surface for the initial oxalic acid concentration  $0.005 \text{ M}$  and photon flux density in the range  $3.26 \times 10^{-10}$  to  $1.07 \times 10^{-8}$  einstein  $\text{cm}^{-2} \text{s}^{-1}$ . An important issue is: under which conditions is the photocatalysis rate controlled by only one of these factors? Table 1 summarizes both experimental (Equation 13) and theoretical (Equation 15) degradation flux densities of oxalic acid, the limiting flux densities of oxygen (Equation 19) and the quantum yields,  $\Gamma$  (%) for different light intensities given by the relation

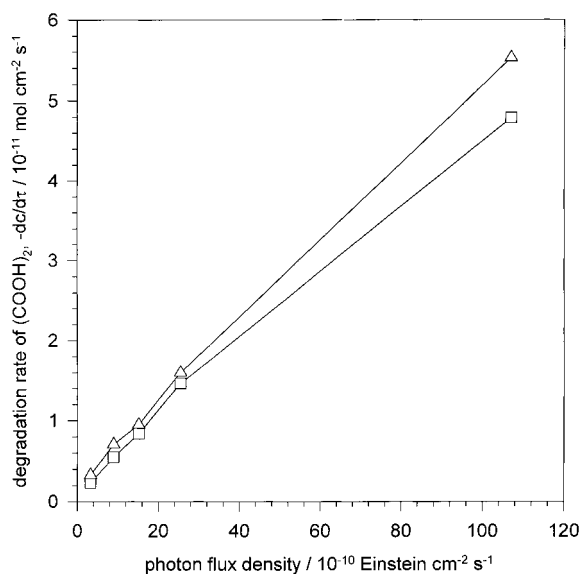


Fig. 4. Effect of flow rate on dependence of the oxalic acid degradation rate,  $dc/d\tau$ , on the photon flux density.  $V_r = 15 \text{ dm}^3$ . Flow rate/ $\text{dm}^3 \text{ min}^{-1}$ : (□) 2.5 and (△) 3.2.

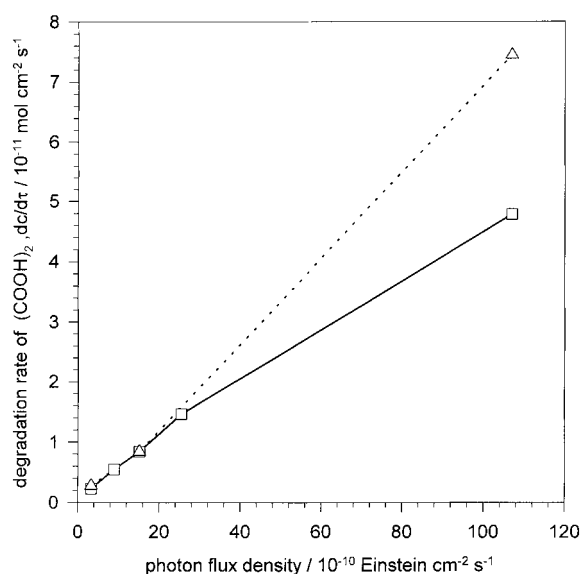


Fig. 5. Effect of oxygen concentration on dependence of the oxalic acid degradation rate,  $dc/d\tau$ , on the photon flux density. Flow rate  $2.5 \text{ dm}^3 \text{ min}^{-1}$ ,  $V_r = 15 \text{ dm}^3$ . Key: (□—□) without oxygen bubbling; (△···△) with oxygen bubbling.

$$\Gamma = 100 \frac{v_{hv}}{v_{org}} \frac{V_r}{J_{hv}A} \frac{dc_{org}}{d\tau} = 200 \frac{V_r}{J_{hv}A} \frac{dc_{org}}{d\tau} \quad (20)$$

It can be seen that the quantum yield decreases with increasing light intensity. This can be attributed to the fact that the number of the electron and hole pairs photogenerated in the semiconductive  $\text{TiO}_2$  particles increases with increasing light intensity, which favours at the same time the recombination against the charge transfer processes.

From Table 1 it is apparent that, while the theoretical degradation flux density does not change with light intensity, since it is given by the limiting flux density of oxygen, the experimental degradation flux density decreases with decreasing light intensity. It can be suggested that the degradation rate is controlled, not only by the oxygen transfer, but also by the photon flux and that the consideration of the three limiting cases, (i), (ii) and (iii), should be corrected. The photometric photon flux irradiating the  $\text{TiO}_2$  surface (significantly higher than the limiting flux of oxygen) leads to the formation of a lower number of charge carrier pairs exploitable for photocatalytic reactions due to the incomplete absorption and recombination. It was assumed in the calculation of limiting cases (i), (ii) and (iii) that the photon flux,  $J_{hv}$ , is equal to the photon flux measured photometrically. In fact this photon flux should be decreased by photons which are not absorbed in the  $\text{TiO}_2$  layer and by the number of charge carrier pairs which undergo recombination.

Equations 16 and 19 describe the theoretical linear dependence of the oxalic acid concentration on the irradiation time for the cases in which the rate determining step is the oxygen flux (16) or photon flux (19). Table 2 shows both experimental (from Fig. 3) and theoretical slopes of the reaction rate,  $dc/d\tau$ .

Table 1. Photocatalytic degradation of oxalic acid under different experimental conditions. Batch mode plate photoreactor with TiO<sub>2</sub> layer (length  $L = 120$  cm, width  $w = 60$  cm), total volume of aqueous solution  $V_r = 15000$  cm<sup>3</sup>, sunbed tubes Osram Eversun L40W/79K, oxygen concentration,  $c_{O_2}^0 = 3.125 \times 10^{-7}$  mol cm<sup>-3</sup>, diffusion coefficient of oxygen,  $D_{O_2} = 2.34 \times 10^{-5}$  cm<sup>2</sup> s<sup>-1</sup>, temperature  $22 \pm 1^\circ$ C

Exp. number	flow rate [dm <sup>3</sup> min <sup>-1</sup> ]	initial concentration of (COOH) <sub>2</sub> × 10 <sup>6</sup> [mol cm <sup>-3</sup> ]	photon flux density × 10 <sup>10</sup> [Einstein cm <sup>-2</sup> s <sup>-1</sup> ]	experimental decomposition flux density of (COOH) <sub>2</sub> × 10 <sup>10</sup> (eq. (13)) [mol cm <sup>-2</sup> s <sup>-1</sup> ]	theoretical decomposition flux density of (COOH) <sub>2</sub> × 10 <sup>10</sup> (eq. (21)) [mol cm <sup>-2</sup> s <sup>-1</sup> ]	theoretical limiting flux density of oxygen × 10 <sup>10</sup> (eq. (15)) [mol cm <sup>-2</sup> s <sup>-1</sup> ]	Quantum yield (eq. (23)) [%]
1	2.5	5.04	3.26	0.231	7.92	3.96	14.2
2	2.5	5.05	8.90	0.548	7.92	3.96	12.3
3	2.5	5.06	15.1	0.840	7.92	3.96	11.1
4	2.5	5.25	25.4	1.46	7.92	3.96	11.5
5	2.5	5.33	107	4.79	7.92	3.96	8.9
6	3.2	5.42	3.26	0.331	8.14	4.07	20.3
7	3.2	5.27	8.90	0.709	8.14	4.07	15.9
8	3.2	5.26	15.1	0.953	8.14	4.07	12.6
9	3.2	5.18	25.4	1.600	8.14	4.07	12.6
10	3.2	5.50	107	5.530	8.14	4.07	10.3
11*	2.5	5.15	3.26	0.281	11.89	5.94**	17.2
12*	2.5	5.44	15.1	0.841	11.89	5.94**	11.1
13*	2.5	5.36	107	7.440	11.89	5.94**	13.9

\*bubbling with oxygen

\*\*oxygen concentration  $4.69 \times 10^{-7}$  mol cm<sup>-3</sup>

Table 2. Theoretical and experimental reaction rates (e.g. slopes  $dc/d\tau$ ) for the photocatalytic degradation of (COOH)<sub>2</sub> for different light intensities (flow rate  $2.5$  dm<sup>3</sup> min<sup>-1</sup>, initial concentration  $0.005$  M)

photon flux density × 10 <sup>10</sup> [Einstein cm <sup>-2</sup> s <sup>-1</sup> ]	theoretical limiting flux density of oxygen × 10 <sup>10</sup> (eq. (15)) [mol]	theoretical slope $dc/d\tau$ in eq. (19) × 10 <sup>-10</sup> [mol cm <sup>-3</sup> s <sup>-1</sup> ]	theoretical slope $dc/d\tau$ in eq. (13) × 10 <sup>-10</sup> [mol cm <sup>-3</sup> s <sup>-1</sup> ]	experimental slope $dc/d\tau$ × 10 <sup>10</sup> eq. (13) [mol cm <sup>-3</sup> s <sup>-1</sup> ]	ratio of teor. (eq. (19)) and experiment slope	ratio of teor. (eq. (22)) and experiment slope
3.26	3.96	-3.80	-0.78	-0.115	33.0	6.8
8.90	3.96	-3.80	-2.14	-0.263	14.4	8.1
15.1	3.96	-3.80	-3.63	-0.403	9.4	9.0
25.4	3.96	-3.80	-6.10	-0.701	5.4	8.7
107	3.96	-3.80	-25.68	-2.30	1.6	11.2

A relatively good agreement can be seen in case (i) (Equation 16) only for the photon flux density  $1.07 \times 10^{-8}$  einstein cm<sup>-2</sup> s<sup>-1</sup> as reported previously [7].

The deviation increases with decreasing photon flux density which indicates that the process is not controlled by oxygen transfer alone but also by the photon flux. In case (iii) (Equation 19) the deviation is caused by incomplete absorption and by recombination of the main part of the photodegraded electrons and holes. If  $J_{hv}$  in Equation 19 were replaced by the corrected photon flux density (the measured photon flux density less the photons not absorbed in the photocatalyst and the number of the recombined electrons and holes) satisfactory agreement between the experimental and calculated slope  $dc/d\tau$  would be expected.

## 5. Conclusion

It was found experimentally that the concentration of oxalic acid decreases linearly during photocatalysis. This confirms that the rate of photocatalysis is controlled by the flux of both oxygen and photons at

higher concentration of oxalic acid ( $\geq 0.005$  M) and photon flux densities in the range  $3.26 \times 10^{-10}$  to  $1.07 \times 10^{-8}$  einstein cm<sup>-2</sup> s<sup>-1</sup>. These two effects act simultaneously and we did not find a region where only one effect was the rate determining step. The influence of oxygen concentration increases with the increasing photon flux which suggests that both effects are mutually combined in the photon flux density range employed. Oxygen can effect the recombination processes due to its reaction with electrons and therefore, at the same time, increase the efficiency of photons absorbed in the TiO<sub>2</sub> particles.

## Acknowledgement

The authors thank the Grant Agency of the Czech Republic for financial support (grant 203/96/0883).

## References

- [1] K. Rajeshwar, *J. Appl. Electrochem.* **25** (1995) 1067.
- [2] H. Gerischer, *Electrochim. Acta* **38** (1993) 3.

- [3] M. R. Hoffman, S. T. Martin, W. Choi and D. W. Bahneman, *Chem. Rev.* **95** (1995) 1.
- [4] M. Trillas, J. Peral and X. Domenech, *Appl. Cat. B; Environ.* **3** (1993) 45.
- [5] C. Kormann, D. W. Bahnemann and M. R. Hoffmann, *Environ. Sci. Technol.* **25** (1991) 494.
- [6] I. M. Butterfield, P. A. Christensen, A. Hamnett, K. E. Shaw, G. M. Walker and S. A. Walker, *J. Appl. Electrochem.* **27** (1997) 385.
- [7] J. Kulas, I. Roušar, J. Krýsa and J. Jirkovský, *J. Appl. Electrochem.* **28** (1998) 843.
- [8] M. A. Fox and M. T. Dulay, *chem. Rev.* **93** (1993) 341.
- [9] D. Bockelmann, 'Photocatalytical Solar Treatment of Waste Water', Ph.D. thesis, Technical University Clausthal, Germany (1993)
- [10] R. W. Mathews, *J. Phys. Chem.* **91** (1987) 3328.
- [11] C. S. Turchi, D. F. Ollis, *J. Phys. Chem.* **92** (1988) 6852.
- [12] R. W. Mathews, *J. Phys. Chem.* **92** (1988) 6853.